

FABRICATED ELECTROMECHANICAL RESONATOR SENSOR FOR LIQUID VISCOSITY MEASUREMENT

Amin Eidi

1) Sahand University of Technology, Tabriz, Iran (✉ a_eidi@sut.ac.ir)

Abstract

The properties of a mechanical resonator provide a valuable ability to measure liquid density and viscosity. The viscosity of liquids is of interest to researchers in both industry and medicine. In this paper, a viscosity sensor for liquids is proposed, which is designed based on an electromechanical resonator. In the proposed sensor, a capacitor is used as an electrostatic actuator. The capacitor is also used to monitor the frequency changes of the proposed resonator. The range of displacement of the resonator and capacitor in response to different fluids under test varies according to their viscosity. The design of the proposed sensor and its electrostatic and mechanical simulations are reported in this paper. Also, the effect of viscosity of several different liquids on its performance has been analyzed and presented experimentally using a prototype.

Keywords: Viscosity sensor, electromechanical resonator, electrostatic simulation, mechanical simulation, sensor fabrication.

© 2023 Polish Academy of Sciences. All rights reserved

1. Introduction

The viscosity of a liquid is important in determining its nature in various industries such as food processing [1]. In medicine, changes in blood viscosity are also symptoms of high blood pressure and heart diseases [2-4]. It has been reported in many works that a liquid has a strong damping effect on the resonator sensor [5-9]. In other words, different damping coefficients of fluids affect mechanical displacement of the resonators.

Many designs have already been introduced as viscosity sensors, indicating high importance of viscosity measurement [10-33]. In previous designs, various methods have been used to measure viscosity, which can be referred to as electrostatic [13], electromagnetic [14], acoustic [15] and thermal [16]. The proposed structures are mainly based on cantilever resonators [17-18]. In previous works, the use of electrostatic measurement method has been introduced as a cheap method [19]. For example, a suitable method has been proposed by measuring the time of the pull-in effect in the electrostatic capacitor for different liquids [20]. Among the different methods, the cheaper method with more accuracy is more desirable.

Many miniaturized viscosity and density resonator sensors suffer from the influence of mounting structures and are fragile or highly temperature dependent [21, 24-25]. Another disadvantage of shear resonance viscosity sensors is the low penetration depth of the generated shear wave [24, 26-28].

The mode of vibration determines the suitability of the resonator for an application. The magnitude of the resonance of the *thickness shear mode* (TSM) quartz crystals depends on the product of the density and viscosity of the liquid [29]. There are some effects that allow separation in principle but with low accuracy [30]. This problem is inherent in any vibration mode where the dominant fluid loading is described by Stokes' second law [31], *e.g.*, in-plane

bending [32] or longitudinal extensional modes [33] of thin beams. The main out-of-plane mode of a cantilever is widely used to circumvent this limitation, as it provides independent responses to density and viscosity. However, viscous losses for out-plane modes may be greater than in-plane modes. It is well established that higher order out-of-plane modes provide better quality factors at intermediate frequencies [34–36].

In this work, a resonator plate in contact with a liquid sample is proposed, and the mechanical displacement amplitude of the plate is different for each sample due to different damping effect of the liquids. This resonator is vibrated using an electrostatic actuator (capacitor) at the desired resonance frequency, and the mechanical displacement of the sensor is measured using the same capacitor.

The proposed sensor design is presented in Sections 2 and 3, the results of its electrostatic and mechanical analyzes based on finite element simulations and experimental results and measurement principle are presented. Sections 4 and 5 present the fabrication process and summarize the contents of this article, respectively.

2. Design of the Proposed Sensor

The proposed sensor is first designed with COMSOL Multiphysics and then evaluated by simulations to optimize it. The proposed viscosity sensor is based on an electromechanical resonator as shown in Fig. 1. This is a simple mechanical resonator that has a suspended plate with 4 folded beam springs.

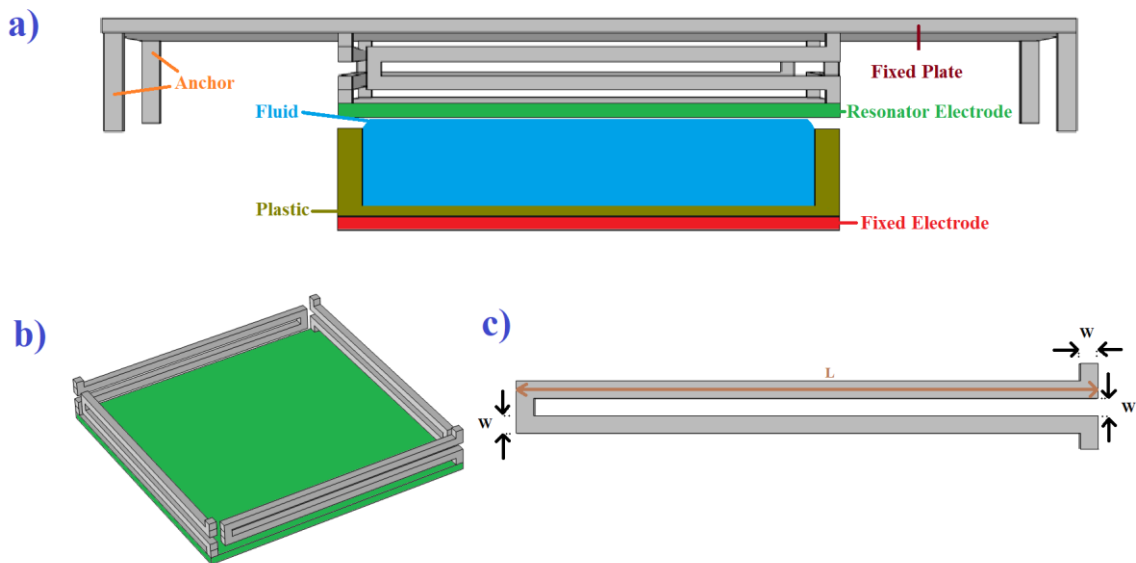


Fig. 1. Design of the proposed sensor. a) Cross view of the sensor with the plastic container and the fluid under test. b) Three-dimensional view of the resonator plate and the springs. c) Cross view of the springs.

The other side of the springs is connected to a large fixed plate and this fixed plate is held by 4 long anchors. There is also a simple capacitive electrostatic actuator, and the suspended plate is the moving electrode of this capacitor. The other fixed electrode of the capacitor is located below the suspended plate and at a distance from it. When the moving plate resonates, its distance from the fixed electrode changes, and the value of the capacitance in this designed capacitor changes according to (1). If this capacitor is excited by a sinusoidal voltage with constant amplitude, the displacement amplitude of the vibrating plate will be constant and the amplitude of the capacitive changes will be constant. In (1), C is the capacitance, A is the contact

area, d is the gap between the capacitor electrodes, ϵ_0 and ϵ_r are the permittivity of free space and relative permittivity of the dielectric material, respectively.

$$C = \frac{\epsilon_0 \epsilon_r A}{d} \quad (1)$$

To test the liquid sample by this sensor, a thin plastic container is required to place the liquid sample inside as shown in Fig. 1. Therefore, between the two electrodes, the capacitor is filled with a thin layer of plastic and the test liquid. Therefore, to test each liquid, the value of the dielectric coefficient of the capacitor will be different. If the material between the two electrodes changes, the dielectric of the capacitor changes and so does the average value of the capacitor. Changes in the viscosity of the liquid cause the moving electrode to face a different restraining force in its path of movement, and this causes the displacement range of the electrode to have a different value due to the change in viscosity. For similar materials or solutions with different percentages under test, the voltage and measurement range must be calibrated at first.

The process of measuring the viscosity of this proposed sensor starts by placing any liquid sample in a container between the two electrodes. Then, the vibration amplitude of the resonator plate is monitored, which depends on the viscosity of the sample as well as its mass. In (2), the viscosity relation of a material in contact with the resonator in the out-of-plane vibration mode (squeeze film mode) is expressed. Therefore, changes in the vibration amplitude of the plate will cause changes in the amplitude of the capacitance changes. Therefore, the amplitude of vibrations of the suspended plate can be calculated and then the viscosity of the tested liquid can be determined by measuring the amplitude of capacitive changes. L_e and H are the length and width of the electrode plates, respectively. Also, b is the damping coefficient of the squeeze film and g_0 is the capacitor gap [37].

$$\eta = \frac{b\pi^4 g_0^3}{384L_e H^3} \quad (2)$$

Each mechanical resonator has several different vibration modes and for the proposed resonator in this sensor, the desired vibration mode is shown in Fig. 2. In this case, all the components of the sensor are selected from polysilicon material and its dimensions are 5 micrometers for W and 200 micrometers for L , respectively, according to Fig. 1. With this specification, the desired vibration mode of the structure emerges at a frequency of 3.28 kHz.

According to (3), the coefficient of springs decreases while their length increases or the number of turns increases or their thickness decreases [38]. In this equation, k is the spring coefficient and E , t , w and l are Young's modulus, thickness, width and length of the beam, respectively. Also, according to (4), by reducing the spring coefficient (k) of the resonator or increasing its mass (M), its vibration frequency (f) decreases [39].

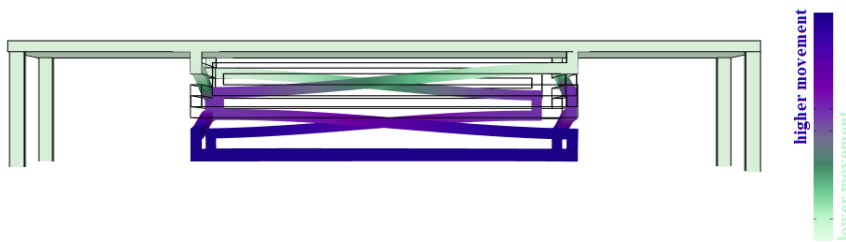


Fig. 2. Desired resonance mode. Resonator plate (moving electrode) vibrates up and down.

$$k_{folded_beam} = \frac{24E}{l_{beam}^3} \cdot \frac{t_{beam} w_{beam}^3}{12} \quad (3)$$

$$f = \frac{1}{2\pi} \sqrt{\frac{k}{M}} \quad (4)$$

The fabricated prototype of the proposed viscosity sensor is illustrated in Fig. 3. Due to the small size of this sensor, it is difficult to take a picture of it. Figure 3 was prepared with the help of slight changes in the emitting light on its different surfaces and by processing its image. Therefore, this image has a suitable contrast for viewing different surfaces of the structure.

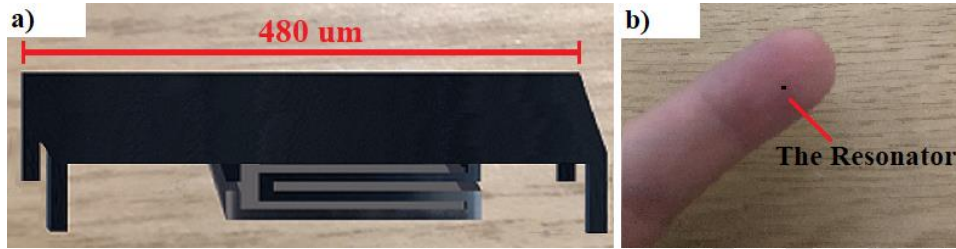


Fig. 3. Prototype of the proposed sensor. (a) Processed image of the prototype resonator using a high resolution camera and image processing methods by MATLAB. (b) Simple image of the resonator to show its scale (Shadows cause it to appear a little bigger than its real size).

It should be noted that in this work, the tested materials are poured into a glass container and a thin and large plate is placed under that container as a fixed electrode. Then the main part of the sensor and the resonator part and the movable electrode are placed inside the container and inside the liquid. Of course, its location in the container is always fixed. In other words, unlike the original design, the sensor is placed inside the sample container in the actual test.

It should also be noted that the anchors of the resonating part have the fixed size. Therefore, the initial distance between the two electrodes is always constant, which is 100 micrometers in the experiments of this work. For accuracy in these tests, the liquid inside the container is filled to a height of 100 micrometers. Also, the glass layer prevents the conduction of liquid between the electrodes.

3. Results

Table 1 lists several different liquids with their relative permittivity and their viscosity calculated using the proposed sensor. It should be noted that for a voltage applied with a constant amplitude to this capacitor, in the vicinity of different materials, a different force will be produced. The amount of the force produced by the capacitor for several different materials at the test site of this sensor according to the results of electrostatic simulations for a voltage of 20 volts is reported in Table 2.

Table 1. List of some materials with their relative permittivity at about 0° C.

| Material | Air | Water | Acetic Acid | Acetylene | Aniline | Olive oil |
|-----------------------|-----|-------|-------------|-----------|---------|-----------|
| Relative Permittivity | 1 | 88 | 4.1 | 1.02 | 7.8 | 3 |

Table 2. Force generated by the electrostatic actuator in the presence of different dielectric materials after applying 20 V on electrodes of the capacitor.

| Material | Air | Water | Acetic Acid | Acetylene | Aniline | Olive oil |
|---------------------------------------|------|-------|-------------|-----------|---------|-----------|
| Generated Force ($\times 10^{-6}$ N) | 0.41 | 33.43 | 1.82 | 0.46 | 3.36 | 1.27 |

The results in Table 2 show that there is no linear relationship between viscosity and the capacitance range. Therefore, the relevant relationships must be accurately equated in the processor to determine the viscosity of the liquid under test in the sensor. This stage of work in the field of data processing was very time consuming. By changing the accuracy of the calculations, the uncertainty estimates in Figure 4 with black dashed lines have been calculated for the results in two limits above and below the average value. In the smaller ranges and by moving away from the central frequency, the number of changes is very small compared to the average value, and the graph related to the estimation of uncertainty is placed on the graph of the average value.

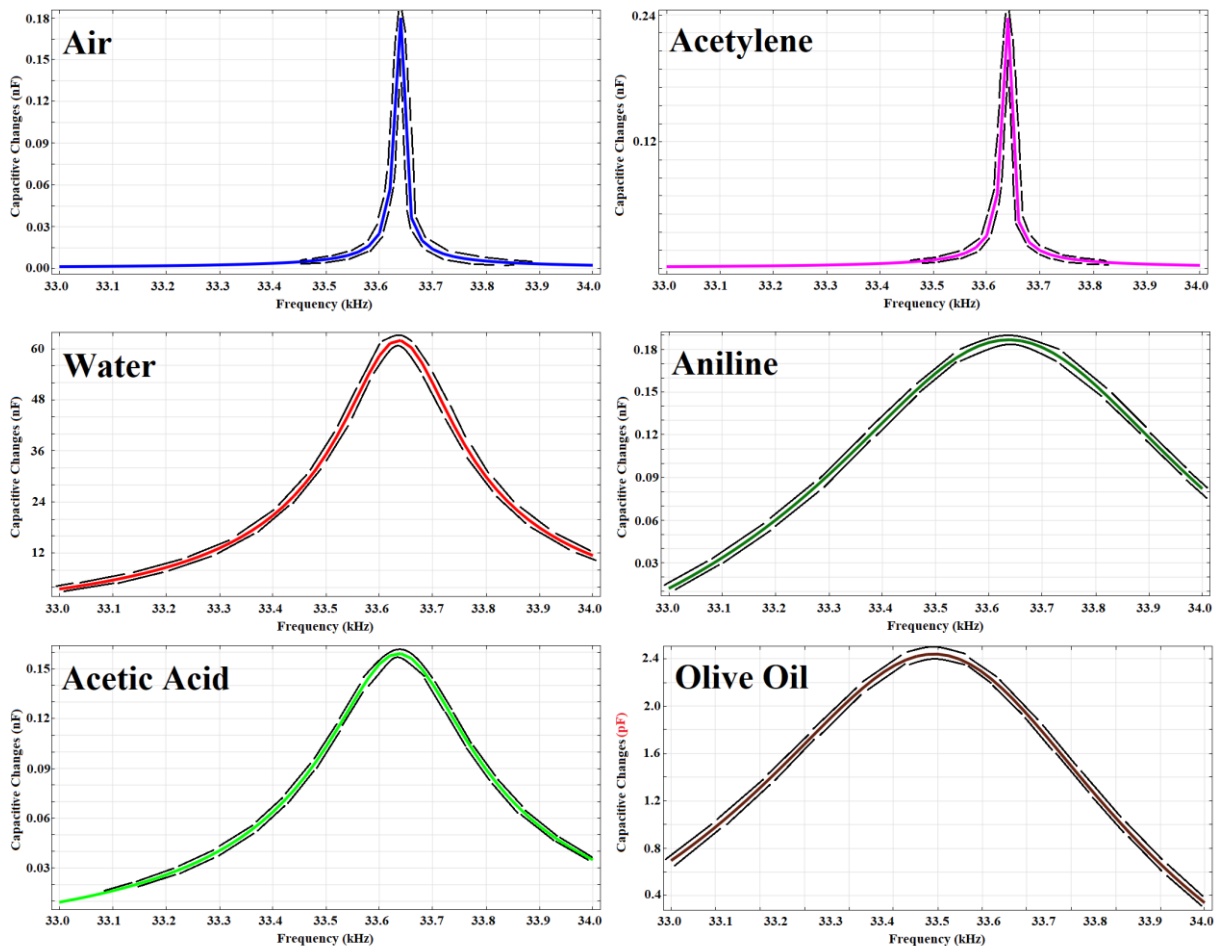


Fig. 4. Frequency response of capacitive changes for different materials.

The relationship between viscosity and resonator vibration amplitude or other parameters is actually not linear. Therefore, below are given explanations on how to determine the viscosity value using the processor's memory.

The output of this sensor can be analyzed with the method based on the resonator quality factor whose formula is written in (5). Q is the resonator quality factor, f_0 is the central frequency and Δf is the bandwidth [40-41]. The frequency response of capacitance changes for fluids in this work is shown in Fig. 4. The amplitude of the frequency responses is increased by an amplifier because in these diagrams the amount of the central frequency and their frequency amplitude are needed to calculate the quality factor of the resonator.

$$Q = \frac{f_0}{\Delta f} \quad (5)$$

The quality factor of the sensor is explained in (6), where m , f and b are the mass of the liquid droplet, the central resonance frequency of the resonator and the damping coefficient, respectively [37]. It should be noted that before measuring the viscosity of a specific liquid, its density and mass can be easily calculated and its value can be replaced in (6). This equation is yields the average displacement of the moving electrode.

$$Q_{squeeze_film} = \frac{2\pi f \cdot m}{b} \quad (6)$$

In Fig. 4, it is clear that the bandwidth of the frequency responses is different for each material, although their central frequencies are very close to each other. It should be noted that these results are obtained for the 100-micrometer gap between the electrodes for the prototype sensor.

In the experimental device, the capacitive sensor amplitude changes in response to different viscosities. Due to the equations above, the viscosity of the tested material can be determined after a certain amount of processing. The output of the viscosity sensor is calculated using the connected processor. With the information obtained from air and water tests with this sensor and knowing their viscosity values, the codes of the AVR processor (ATmega32) are set. Actually, the sensor output shown on the display for water and air is calibrated by the processor codes.

To measure the viscosity of the liquid substance with the help of the proposed sensor, the frequency response of the capacitance changes in the proposed resonator is considered. Assuming that the central frequency of the designed resonator is already known, the capacitive sensor is designed in the same range when recording the output signal. Also, with the help of an intermediate analog filter, high and low frequency noises in the output of the designed capacitor are removed and the filtered signal is transmitted to the processor.

Then, the amplitude and the frequency response of the sensor are calculated with the calibrated codes of the processor for each tested material. According to the numbers obtained for the bandwidth and amplitude of capacitance changes by the processor, with the help of the information table in the processor's memory and according to the coded relationships, the viscosity value for a material is determined. According to these details, the data is loaded on the processor after precise calibration.

After that, tests were performed for acetic acid, acetylene, aniline and olive oil. The output of the sensor presented in Table 3. By comparing the values obtained in these tests with the proposed sensor, it can be seen that they are close to real viscosity of these materials. Viscosity of the referenced materials in Table 3 is reported in previous works. Viscosity of olive oil [42], aniline [43], acetylene [44] and acetic acid [45] is reported using other methods in Table 3 and compared with the proposed sensor results.

Table 3. List of some materials with their viscosity. The air and water viscosity used to calibrate the proposed sensor according to results of previous works. The viscosity of other materials is determined using the prototype sensor of this work.

| Material | Air | Water | Acetic Acid | Acetylene | Aniline | Olive oil |
|---|-------|-------|-------------|-----------|---------|-----------|
| Central Resonance Frequency (kHz) | 33.63 | 33.64 | 33.64 | 33.63 | 33.65 | 33.85 |
| Viscosity ($\mu\text{Pa.S}$) – from the proposed sensor | 18.1 | 890 | 1120 | 9.40 | 2908 | 34000 |
| Test Temperature ($^{\circ}\text{C}$) | 25 | 25 | 25 | 25 | 22 | 40 |
| Viscosity ($\mu\text{Pa.S}$) – from previous works | 18.1 | 890 | 1130 | 9.43 | 2912 | 34400 |

Viscosity, which changes the scope of resonator damping effect, also changes the amount of central resonance frequency. Therefore, in these tests for each material, the frequency of the voltage source is manually changed to such an extent so that the capacitance changes shown on the oscilloscope appear with a larger amplitude. In this work, the central resonance frequency of the resonator was also recorded in each test for each material and reported in Table 3.

Now, after studying the relationships and the overall performance of the proposed sensor, it is necessary to pay attention to how to calculate the viscosity of the liquid sample once again according to the previous equations. By obtaining the frequency response characteristics of capacitive changes, the quality factor of the proposed resonator is calculated according to (5). By putting this value of the quality factor in (6), the value of the damping factor for the corresponding test is calculated. Then, by putting the value of the damping coefficient in (2), the viscosity value for the tested liquid is determined. These calculations were performed using a microprocessor in the experiments and the results are reported according to Table 3.

When the purpose is to determine the viscosity of similar materials, the appropriate voltage for the actuator (capacitor) must be selected. The voltage value should not be so high that the resonator plate is connected to the bottom of the container and should not be so low that the amplitude of displacements cannot be measured.

4. Fabricating Process

To fabricate the resonator, which is the main part of the proposed sensor, the polysilicon and photoresist are deposited several times in a specific order according to the design. Figure 5 illustrates the iterative process that provides the fabrication of the resonator. The first layer is polysilicon and the following steps are repeated in the Fig. 5 stage. The number of steps below is written on the stages of the figure which are used at each stage.

- 1) Deposition and patterning of the photoresist.
- 2) Deposition of polysilicon.
- 3) Removing the photoresist with acid.

From (a) to (u) the steps above are repeated 7 times. If the Fig. 5 (u) is rotated 180 degrees, the shape of the proposed sensor in the Fig. 3 can be seen easily. In Fig. 5 (d), (j) and (p), deposition and patterning of the photoresist were performed twice to form the photoresist on two levels.

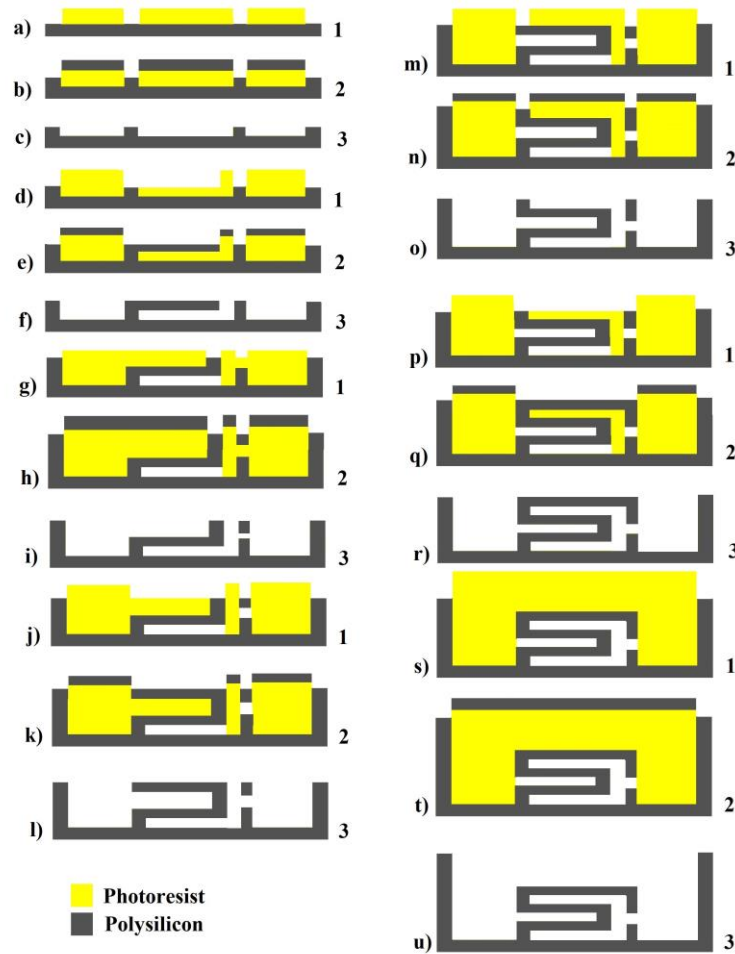


Fig. 5. Fabrication process of the resonator of the proposed sensor. Numbers (1), (2) and (3) in front of each part of the figure indicate the operation of the fabrication process. Number (1) means depositing and patterning of the photoresist, Number (2) indicates depositing of polysilicon, and number (3) refers to removing of the photoresist.

5. Conclusions

In this paper, a viscosity sensor based on an electromechanical resonator is proposed that shows significant changes in the displacement amplitude of the resonator plate in response to the viscosity of different materials. This sensor can be made in different dimensions and with different materials according to the specific purpose, and its operating frequency can be adjusted by changing the mass values and resonating springs to a certain degree to determine the viscosity of other material in different ranges. This sensor can be used in the food industry to evaluate the viscosity of liquids such as milk. Also, it can be used to calculate blood viscosity in medical diagnostic tools. According to the results of Table 3 and comparing the viscosity of materials which are measured using the proposed sensor with the values which are reported in previous works, the error is lower than 0.015 %, *i.e.*, it is negligible.

In the proposed sensor, the changes in the vibration amplitude of the resonator plate are converted into capacitance changes and the sensor output is recorded with a low-cost method. An automatic voltage source can be added to complement this sensor as a commercial sensor. Within a given range, its frequency can be automatically controlled by a processor to provide a suitable frequency for the voltage proportional to the amount of damping effect for each liquid under test.

References

- [1] Kassim, M. S., & Sarow, S. A. (2020). Flows of Viscous Fluids in Food Processing Industries: A review. *IOP Conference Series: Materials Science and Engineering* (Vol. 870, No. 1, p. 012032). IOP Publishing. <https://doi.org/10.1088/1757-899X/870/1/012032>
- [2] Yildirim, C., Şenyol, A. M., & Kamber, D. (2001). Blood viscosity and blood pressure: role of temperature and hyperglycemia. *American Journal of Hypertension*, 14(5), 0–438, [https://doi.org/10.1016/s0895-7061\(00\)01260-7](https://doi.org/10.1016/s0895-7061(00)01260-7)
- [3] Chen, G., Zhao, L., Liu, Y. W., Liao, F. L., Han, D., & Zhou, H. (2012). Regulation of blood viscosity in disease prevention and treatment. *Chinese Science Bulletin*, 57(16), 1946–1952, <https://doi.org/10.1007/s11434-012-5165-4>
- [4] Sun, G., Yang, L., Wang, W., Zhang, S., Luo, Z., Wu, G., Liu, X., Hao, D., Yang, Y., & Li, X. (2020). An Algorithm for the Noninvasive and Personalized Measurement of Microvascular Blood Viscosity Using Physiological Parameters. *BioMed Research International*, 2020, 1–7, <https://doi.org/10.1155/2020/7013212>
- [5] Surabhi, J., Sherman, H., & Srikar, V. (2014). Design strategies for controlling damping in micromechanical and nanomechanical resonators. *EPJ Techniques and Instrumentation*, 1(1), 1-14. <https://doi.org/10.1140/epjt5>
- [6] Won, D.-J., Lee, S., & Kim, J. (2020). Analysis of liquid-type proof mass under oscillating conditions. *Micro and Nano Systems Letters*, 8(1), 1–7. <https://doi.org/10.1186/s40486-020-00115-y>
- [7] Zhang, K., Chen, Z., Zhu, Q., Jiang, Y., Liu, W., & Wu, P. (2018). Damping Force and Loading Position Dependence of Mass Sensitivity of Magnetoelastic Biosensors in Viscous Liquid. *Sensors*, 19(1), 1-9, <https://doi.org/10.3390/s19010067>
- [8] Eidi, A., Badri-Ghavifekr, H., & Shamsi, M. (2019). A Novel Biosensor Based on Micromechanical Resonator Array for Lab-On-a-Chip Applications. *Sensing and Imaging*, 20(1), 1-10, <https://doi.org/10.1007/s11220-019-0261-z>
- [9] Eidi, A., Shamsi, M., & Badri-Ghavifekr, H. (2022). Design and evaluation of a micro resonator structure as a biosensor for droplet analysis with a standard fabrication method. *Sensor Review*, 42(2), 263-273. <https://doi.org/10.1108/SR-07-2021-0209>
- [10] Eidi, A. (2022). Optimized cantilever sensor based on parallel high dielectric material. *Sensing and Imaging*, 23(1), 1-10. <https://doi.org/10.1007/s11220-022-00381-7>
- [11] Eidi, A. (2022). An Ultra-Low Frequency and Low-Pressure Capacitive Blood Pressure Sensor Based on Micro-Mechanical Resonator. *Sensing and Imaging*, 23(35), 1-10. <https://doi.org/10.1007/s11220-022-00398-y>
- [12] Eidi, A. (2023). Modeling and simulation of an ultra-low frequency and low-pressure resonator. *COMPEL- The international journal for computation and mathematics in electrical and electronic engineering*, 42(2), 673-684. <https://doi.org/10.1108/COMPEL-07-2022-0239>
- [13] Arsenjuk, L., Wieseahn, M., Zimmermann, E. M., Katschan, W., & Agar, D. W. (2020). Capacitive determination of wall-film thickness in liquid-liquid slug flow and its application as a non-invasive microfluidic viscosity sensor. *Sensors and Actuators A: Physical*, 315, 112342. <https://doi.org/10.1016/j.sna.2020.112342>
- [14] Heinisch, M., Voglhuber-Brunnmaier, T., Reichel, E. K., Dufour, I., & Jakoby, B. (2015). Electromagnetically driven torsional resonators for viscosity and mass density sensing applications. *Sensors and Actuators A: Physical*, 229, 182-191. <https://doi.org/10.1016/j.sna.2015.03.033>
- [15] Abdallah, A., Heinisch, M., & Jakoby, B. (2013). Measurement error estimation and quality factor improvement of an electrodynamic-acoustic resonator sensor for viscosity measurement. *Sensors and Actuators A: Physical*, 199, 318-324. <https://doi.org/10.1016/j.sna.2013.05.033>
- [16] Brouwer, M. D., Gupta, L. A., Sadeghi, F., Peroulis, D., & Adams, D. (2012). High temperature dynamic viscosity sensor for engine oil applications. *Sensors and Actuators A: Physical*, 173(1), 102-107. <https://doi.org/10.1016/j.sna.2011.10.024>
- [17] Cakmak, O., Ermeke, E., Kilinc, N., Yaralioglu, G. G., & Urey, H. (2015). Precision density and viscosity measurement using two cantilevers with different widths. *Sensors and Actuators A: Physical*, 232, 141–147. <https://doi.org/10.1016/j.sna.2015.05.024>

- [18] Sathiya, S., & Vasuki, B. (2016). A structural tailored piezo actuated cantilever shaped 2-DOF resonators for viscosity and density sensing in liquids. *Sensors and Actuators A: Physical*, 247, 277–288. <https://doi.org/10.1016/j.sna.2016.05.052>
- [19] Tröls, A., Clara, S., & Jakoby, B. (2016). A low-cost viscosity sensor based on electrowetting on dielectrics (EWOD) forces. *Sensors and Actuators A: Physical*, 244, 261–269. <https://doi.org/10.1016/j.sna.2016.04.047>
- [20] Dias, R. A., de Graaf, G., Wolffenbuttel, R. F., & Rocha, L. A. (2014). Gas viscosity sensing based on the electrostatic pull-in time of microactuators. *Sensors and Actuators A: Physical*, 216, 376-385. <https://doi.org/10.1016/j.sna.2014.05.004>
- [21] Heinisch, M., Reichel, E. K., Dufour, I., & Jakoby, B. (2012). Tunable resonators in the low kHz range for viscosity sensing. *Sensors and Actuators A: Physical*, 186, 111-117. <https://doi.org/10.1016/j.sna.2012.03.009>
- [22] Sparks, D., Smith, R., Cruz, V., Tran, N., Chimbayo, A., Riley, D., & Najafi, N. (2009). Dynamic and kinematic viscosity measurements with a resonating microtube. *Sensors and Actuators A: Physical*, 149(1), 38-41. <https://doi.org/10.1016/j.sna.2008.09.013>
- [23] Heinisch, M., Voglhuber-Brunmaier, T., Reichel, E. K., Dufour, I., & Jakoby, B. (2014). Reduced order models for resonant viscosity and mass density sensors. *Sensors and Actuators A: Physical*, 220, 76-84. <https://doi.org/10.1016/j.sna.2014.09.006>
- [24] Jakoby, B., Beigelbeck, R., Keplinger, F., Lucklum, F., Niedermayer, A., Reichel, E. K., Riesch, C., Voglhuber-Brunmaier, T., & Weiss, B. (2010). Miniaturized sensors for the viscosity and density of liquids-performance and issues. *IEEE Transactions on Ultrasonics, Ferroelectrics and Frequency Control*, 57(1), 111–120. <https://doi.org/10.1109/TUFFC.2010.1386>
- [25] Hannes, A., Stefan, C., Roman, B., Samir, C., Franz, K., & Bernhard, J. (2012). Sensing the characteristic acoustic impedance of a fluid utilizing acoustic pressure waves. *Sensors and Actuators A: Physical*, 186, 94-99. <https://doi.org/10.1016/j.sna.2012.02.050>
- [26] Kanazawa, K. K., & Gordon, J. G. (1985). Frequency of a quartz microbalance in contact with liquid. *Analytical Chemistry*, 57(8), 1770–1771. <https://doi.org/10.1021/ac00285a062>
- [27] Riesch, C., Jachimowicz, A., Keplinger, F., Reichel, E. K., & Jakoby, B. (2008, October). A micromachined doubly-clamped beam rheometer for the measurement of viscosity and concentration of silicon-dioxide-in-water suspensions. In *SENSORS, 2008 IEEE* (pp. 391-394). IEEE. <https://doi.org/10.1109/icsens.2008.4716461>
- [28] Reichel, E. K., Riesch, C., Keplinger, F., Kirschhock, C. E., & Jakoby, B. (2010). Analysis and experimental verification of a metallic suspended plate resonator for viscosity sensing. *Sensors and Actuators A: Physical*, 162(2), 418-424. <https://doi.org/10.1016/j.sna.2010.02.017>
- [29] Martin, S. J., Granstaff, V. E., & Frye, G. C. (1991). Characterization of a quartz crystal microbalance with simultaneous mass and liquid loading. *Analytical Chemistry*, 63(20), 2272-2281. <https://doi.org/10.1021/ac00020a015>
- [30] Abdallah, A., Reichel, E. K., Voglhuber-Brunmaier, T., Heinisch, M., Clara, S., & Jakoby, B. (2015). Symmetric mechanical plate resonators for fluid sensing. *Sensors and Actuators A: Physical*, 232, 319-328. <https://doi.org/10.1016/j.sna.2015.05.022>
- [31] Matsiev, L. F. (1999, October). Application of flexural mechanical resonators to simultaneous measurements of liquid density and viscosity. In *1999 IEEE Ultrasonics Symposium. Proceedings. International Symposium* (Cat. No. 99CH37027) (Vol. 1, pp. 457-460). IEEE. <https://doi.org/10.1109/ULTSYM.1999.849439>
- [32] Kucera, M., Wistrela, E., Pfusterschmied, G., Ruiz-Díez, V., Manzanque, T., Hernando-García, J., Sánchez-R., José L., Jachimowicz, A., Schalko, J., Bittner, A., & Schmid, U. (2014). Design-dependent performance of self-actuated and self-sensing piezoelectric-AlN cantilevers in liquid media oscillating in the fundamental in-plane bending mode. *Sensors and Actuators B: Chemical*, 200, 235–244. <https://doi.org/10.1016/j.snb.2014.04.048>
- [33] Toledo, J., Manzanque, T., Hernando-García, J., Vázquez, J., Ababneh, A., Seidel, H., Lapuerta, M., & Sánchez-Rojas, J. L. (2014). Application of quartz tuning forks and extensional microresonators for viscosity and density measurements in oil/fuel mixtures. *Microsystem Technologies*, 20(4-5), 945–953. <https://doi.org/10.1007/s00542-014-2095-x>

- [34] Van E., Cornelis A., & Sader, J. E. (2007). Frequency response of cantilever beams immersed in viscous fluids with applications to the atomic force microscope: Arbitrary mode order. *Journal of Applied Physics*, 101(4), 44908 <https://doi.org/10.1063/1.2654274>
- [35] Wilson, T. L., Campbell, G. A., & Mutharasan, R. (2007). Viscosity and density values from excitation level response of piezoelectric-excited cantilever sensors. *Sensors and Actuators A: Physical*, 138(1), 44-51. <https://doi.org/10.1016/j.sna.2007.04.050>
- [36] Ghatkesar, M. K., Braun, T., Barwich, V., Ramseyer, J-P., Gerber, C., Hegner, M., & Lang, H. P. (2008). Resonating modes of vibrating microcantilevers in liquid. *Applied Physics Letters*, 92(4), 043106. <https://doi.org/10.1063/1.2838295>
- [37] Lin, A. T., Yan, J., & Seshia, A. A. (2009, September). Dynamic response of water droplet coated silicon MEMS resonators. In *2009 IEEE International Ultrasonics Symposium* (pp. 669-672). IEEE. <https://doi.org/10.1109/ultsym.2009.5441588>
- [38] Wai-Chi, W., Azid, A. A., & Majlis, B. Y. (2010). Formulation of stiffness constant and effective mass for a folded beam. *Archives of Mechanics*, 62(5), 405-418.
- [39] Alster, M. (1972). Improved calculation of resonant frequencies of Helmholtz resonators. *Journal of Sound and Vibration*, 24(1), 63-85. [https://doi.org/10.1016/0022-460x\(72\)90123-x](https://doi.org/10.1016/0022-460x(72)90123-x)
- [40] Liu, Y., Wang, D., & Wang, D. F. (2017). Analytical study on effect of piezoelectric patterns on frequency shift and support loss in ring-shaped resonators for biomedical applications. *Microsystem Technologies*, 23(7), 2899-2909. <https://doi.org/10.1007/s00542-016-3112-z>
- [41] Srikar, V. T., & Senturia, S. D. (2002). Thermoelastic damping in fine-grained polysilicon flexural beam resonators. *Journal of Microelectromechanical Systems*, 11(5), 499-504. <https://doi.org/10.1109/JMEMS.2002.802902>
- [42] Fellows, P. J. (2009). *Food Processing Technology: Principles and Practice* (3rd ed.). Woodhead Publishing.
- [43] Steiner, L. A. (1938). Viscosity of Aniline between 20° and 100° C. *Industrial & Engineering Chemistry Analytical Edition*, 10(10), 582-584. <https://doi.org/10.1021/ac50126a004>
- [44] Bailey, B. J. (1970). The viscosity of carbon dioxide and acetylene at atmospheric pressure. *Journal of Physics D: Applied Physics*, 3(4), 550. <https://doi.org/10.1088/0022-3727/3/4/312>
- [45] Bleazard, J. G., Sun, T. F., & Teja, A. S. (1996). The thermal conductivity and viscosity of acetic acid-water mixtures. *International Journal of Thermophysics*, 17, 111-125. <https://doi.org/10.1007/BF01448214>



Amin Eidi was born in Tabriz, Iran in 1994. He received the M.Sc. (2018) and Ph.D. (2022) degree from Sahand University of Technology (SUT), Iran. He is currently a researcher and lecturer at the Faculty of Biomedical Engineering of SUT.